Investigating metrics based on Phase variance for atmospheric turbulence effects on a 10km Laser beam propagation path

Diego A. Lozano Jimenez
MS Candidate, Department of Mechanical Engineering, University of Texas at El Paso
500 W. University, EL Paso TX 79968

Dr. Vinod Kumar
Associate Professor, Department of Mechanical Engineering, University of Texas at El Paso
500 W. University, EL Paso TX 79968

Dr. V.S. Rao Gudimetla
Senior Research Physicist, AFRL, 550 Lipoa Parkway, Kihei, HI 96753

ABSTRACT

Laser beam propagation through atmospheric turbulence is investigated using the phase screen approach with the von Kármán refractive power spectral density. For simplicity, plane wave propagation through a 10,000m long atmospheric horizontal path is considered. Statistical analysis of the phase information at the output signal and related metrics are examined. Initial phase screen values are observed to be discontinuous and, therefore, unwrapped using 2D Goldstein branch cut phase unwrapping algorithm to remove the unphysical discontinuities. Statistical parameters such as phase variance, autocorrelation and structure function are calculated to describe the random behavior of phase. At high turbulence, simulated values are well below the theoretical approximations due to limitations within the simulation. Phase information can characterize atmospheric effects on laser propagation over a long path but further investigations are needed to establish the use of phase data at deep turbulence.

1 INTRODUCTION

There is an expanding interest in characterizing atmospheric turbulence effects on laser beams propagating over a long path for directed energy applications. For optical systems, lasers propagating long distances lose their coherence due to the fluctuations in the refractive index. A dominant cause for the refractive index fluctuations, can be attributed to cumulative effect of turbulent eddies present in the atmosphere along the laser beam propagation path. Current analysis of atmospheric turbulence effects is based on theoretical and statistical models [1]–[3] derived from the Kolmogorov approach. Supporting experimental evidence [4]–[6] helped validate the classical theory of optical propagation. Inaccuracies develop when implementing this model for various conditions like long range propagation, deep atmospheric turbulence, or a combination of both showing experimental results that deviate from the theory. While Kolmogorov approach is still used for long path propagation, further investigation is needed to comprehend its limitations and determine parameters that can describe deep turbulence effects.

2 METHODOLOGY

Atmospheric turbulence is caused by the large-scale variations of temperature in the air. Temperature variations generate wind. Strong wind can transition laminar flow to turbulent flow. In turbulent flow, air at different temperatures begin to mix producing randomly distributed pockets of air that vary in size called eddies. Attempting to numerically solve turbulent flow can be difficult and computationally taxing, especially for the case of deep turbulence. To characterize atmospheric turbulence in this study, the Kolmogorov approach is implemented to statistically model the effects of eddies. Kolmogorov model proposes that the kinetic energy of a turbulent flow is transmitted from the larger eddies into smaller eddies.

The energy cascade theory begins with eddies the size equal to that of the outer scale length L_o. The input energy is then progressively divided and redistributed into smaller eddies until the eddies are equal, in size, to the inner scale length l_o (Figure 1). Eddies within this inertial range are assumed to be statistically homogeneous and isotropic.

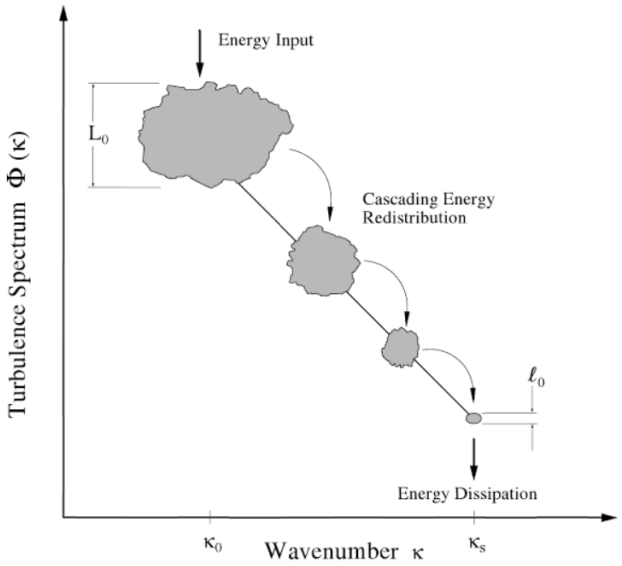

Figure 1: Description of Kolmogorov Energy Cascade Theory [6]

In this subrange of local homogeneity, Kolmogorov [1] considered the difference between two velocity points to be statistically dependent on the displacement vector separating them. The assumption led him to develop the statistical structure of turbulence that can be described by a single structure function. This theory only holds true for displacement vectors between the outer-inner scale lengths.

2.1 Optical Turbulence and Associated Parameters

Tatarskii [3], [7] proved, with the concept of conservative passive additives, that the refractive index fluctuations obey the same structure function law as velocity and temperature turbulence. In doing so we calculate the refractive index structure constant C_n^2

$$C_n^2 = \left(\frac{79 \times 10^{-8}\, P}{T^2}\right)^2 C_T^2$$

where P is atmospheric pressure, T is air temperature, and $C_T^2$is the structure function parameter for temperature. The typical range of values for C_n^2 are between (10^{-13} - 10^{-17} $m^{-2/3}$). After deriving the structure function for the refractive index, we can determine the spectral density function $\Phi_n(\kappa)$ in term of Kolmogorov's inertial subrange model (Tatarskii [3] and Strohbehn [8]).

$$\phi_n(\kappa)\frac{1}{4\pi^2\kappa^2}\int_0^\infty \frac{sin(\kappa r)}{\kappa r}\frac{d}{dr}\left[r^2\frac{d}{dr}D_n(r)\right]dr \; = 0.033C_n^2\kappa^{-11/3}$$

There are other models for the refractive power spectral density. For our study, we will be using the von Kármán to include the outer-scale effects.

$$\Phi_n^{vk}(\kappa) = \frac{0.033C_n^2}{(\kappa^2+\kappa_0^2)^{11/6}} \quad for \;\; 0 \le \kappa \ll 1/l_o$$

where $\kappa = 2\pi\left(f_x\hat{\imath} + f_y\hat{\jmath}\right)$ is the angular spatial frequency in rad/m, C_n^2 is the refractive index structure constant and $\kappa_0 = 2\pi/L_0$.

3 PROBLEM STATEMENT

In this study, the Rytov index will be used to represent the intensity of the atmospheric turbulence. Rytov is the log-amplitude fluctuations for the plane wave and is given by $\sigma_\chi^2 = 0.312C_n^2k^{7/6}L^{11/6}$ for Kolmogorov spectra.

3.1 Prior Work

In the summer 2016 USAF SFFP report [9], the turbulence intermittency was studied for the turbulence effects. It was modeled through non-Kolmogorov methods using fractal descriptions of eddies that incorporate space filling concepts present in the inertial turbulence ranges. The main objectives of the research were to examine the impact on intensity variance and total number of zero intensity points in the outputs with respect to the Rytov index and the power law exponent. The study showed that the variance of intensity increased linearly approximately four times the Rytov value for the case of weak turbulence. The theory broke down at high turbulence as the variance of intensity drastically increased at Rytov=0.5 before saturating at around Rytov=1. Further investigations however are needed to establish stronger correlations between eddies' characteristics in deep turbulence and high order statistics for the beam propagation.

3.2 Simulations

As an extension to the previous study[9], statistical analysis of the phase information at the output signal is examined through the Kolmogorov spectrum. For simplicity, we consider a plane wave propagating through a 10km path with a constant C_n^2. The inner and outer scale lengths are 5mm and 10m respectively. All simulations are carried for a 2048x2048 number of samples N, with a 5mm grid spacing interval δ, using Fresnel Propagation [10].

$$U(x_2,y_2) = \frac{e^{ik\Delta z}}{i\lambda\Delta z}\iint_{-\infty}^{\infty} U(x_1,y_1)e^{i\frac{k}{2\Delta z}(x_1x_2+y_1y_2)}dx_1dy_1$$

To introduce atmospheric turbulence, the propagation distance is subdivided into slabs of distance Δz (Figure 2-right). Within z , the plane wave is propagated linearly using Fresnel propagation in a vacuum. Atmospheric turbulence is introduced at the end of the partial propagation distance (Figure 2, Left). The propagated wave phase is altered by introducing a turbulent-induced phase term to the phase of the propagated wave in the Fourier domain.

Therefore, the relationship between the phase spectrum for each screen and refractive-index is $\Phi_\phi(\kappa) = 2\pi^2 k^2 \Delta z \Phi_n^{vk}(\kappa)$.

Phase screen simulations are based on the Fresnel propagation, refractive index power-spectrum and computer-generated random numbers to obtain a random field. These values are then implemented into two-dimensional arrays of phase values on a grid of sample points that have the same statistical values as turbulence-induced phase variations [10].

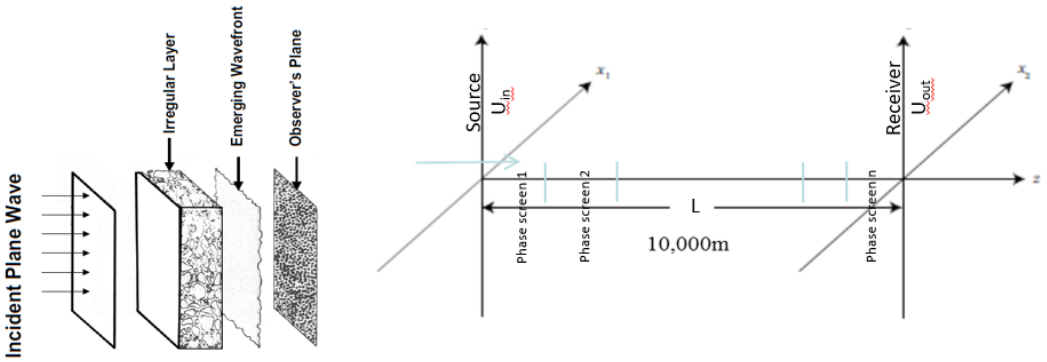

Figure 2: Plane beam propagation schematic

Propagation of the wave field from screen to screen can be written as

$$U = U_0 e^{-i\psi}$$

where U_0 is the solution to the Fresnel propagation in a vacuum of a distance Δz and ψ is the complex phase perturbation. The procedure is repeated for all screens until the plane wave reaches the receiver plane. The simulations are performed using 15 screens over a 10km propagation path, i.e., spacing between screens is 666.6m. Figure 3 presents results for the intensity, wrapped and unwrapped phase of the propagated wave at the receiver plane.

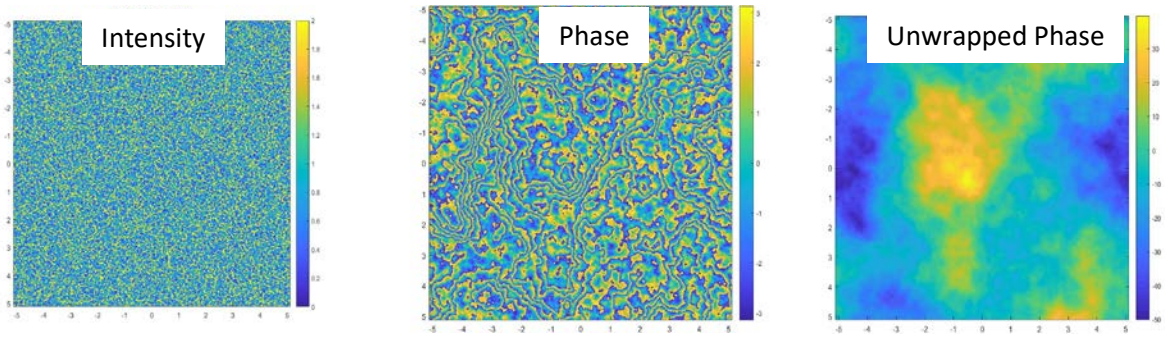

Figure 4: Phase screen simulated results

The phase images that are produced by the plane wave propagating through a turbulent medium have discontinuities (Figure 4-middle). The built-in Matlab version of 2D unwrap function embedded in MATLAB fails to smoothen the discontinuities for strong turbulent cases.

A more robust unwrap scheme is developed to perform statistical calculations of the phase data. The scheme is based on the 2D Goldstein branch cut phase unwrapping algorithm [11], [12], compiled by *Bruce Spottiswoode* and edited by *Carey Smith* [13].

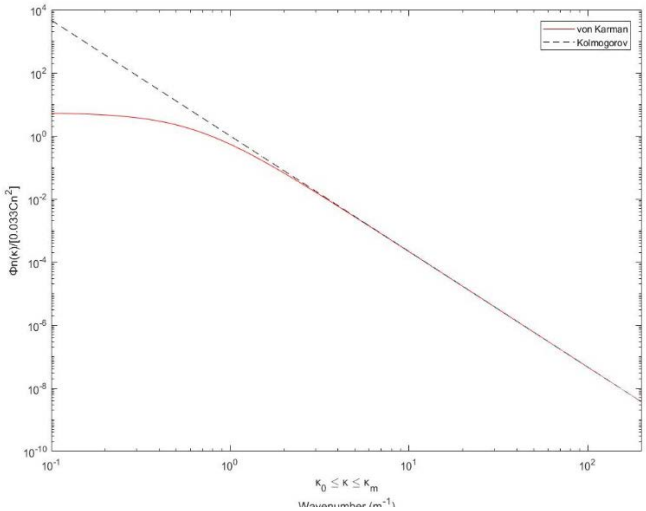

Figure 4: Effects of Large Eddies on the power spectrum

We take the unwrapped phase screens to compute the phase variance. Phase varianace is sensitive to the small-wavenumber portion of the spectrum of irregularities and is also dependent on outer scale length, the region where energy is fed into the Kolmogorov energy cascade process. In order to demonstrate the outer scale effects on the phase variance, an approximation provided by *Wheelon* [6] as a function of the von Kármán power spectrum is used and is given as $\langle\varphi^2\rangle = 0.782Lk^2C_n^2\kappa_0^{-5/3}$ where $k = 2\pi/\lambda$.

Like the power spectral density (Figure 4), phase variance expression is primarily determined by the largest eddies. This is important for optics applications because if measured values of L, k, C_n^2 and $\langle\varphi^2\rangle$ are known, then we can establish a distribution of outer scale lengths. Determining phase variance can therefore help us to understanding outer scale effects of the atmospheric turbulence. If the simulated phase variance values are validated with the theoretical approximation by determining the phase structure function that obeys the same structure function law as the refractive index.

$$D_\varphi(\rho) = \langle(\varphi_1 - \varphi_2)^2\rangle = 2[\langle\varphi^2\rangle - \langle\varphi_1\varphi_2\rangle] = 2\big[\Gamma_{\varphi\varphi}(0) - \Gamma_{\varphi\varphi}(\rho)\big]$$

The phase structure function is another statistical measure to describe the random behavior of phase values, and is closely related to the phase auto-correlation. Determining the autocorrelation is often too difficult to compute in the spatial domain but is equivalent to simple multiplication in the frequency domain.

$$\Gamma_{\varphi\varphi}(\rho) = \mathcal{F}^{-1}\{\mathcal{F}[\varphi(r)]\mathcal{F}[\varphi(r)]^*\}$$

The notation * is the complex conjugate of the function and $\rho = |r_1 - r_2|$ is the scalar separation. This will allow for a straight forward approach in determining the phase structure function in the 2-D case.

4 RESULTS AND DISCUSSIONS

Calculations show that theoretical phase variance approximation linearly increases with respect to Rytov if C_n^2, L, k, and L_o are known. Note that these results were obtained for 20 trials within the simulation at relatively smaller grid size (2048x2048) which may not be sufficient.

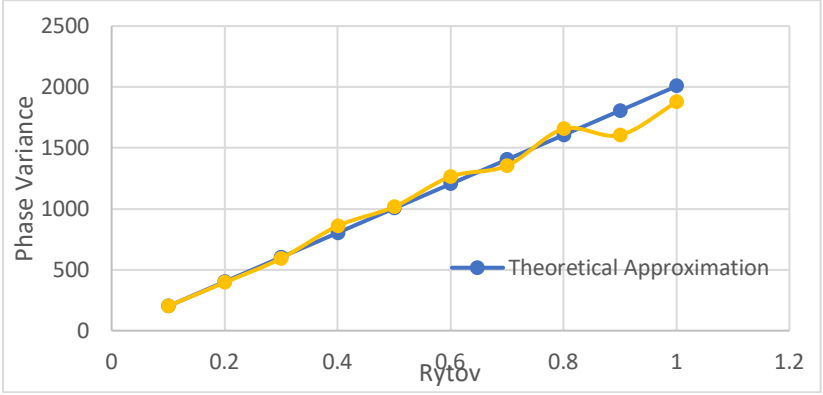

Figure 5: Phase variance at the receiving end in comparison to theoretical approximations

The phase variance at the receiver plane shows a linear trend with respect to the Rytov index with small variations from the theoretical values. Limitations appear at high turbulence (Rytov>0.9) as the phase variance is less than the theoretical approximation. This can be attributed to the finite spatial dynamic range imposed by the maximum available grid size. This is because the von Kármán power spectrum has more influence in low spatial frequencies (Figure 3). The spatial phase screen size needs to be significantly larger so the sample frequency spacings can be low enough to accurately represent the outer scale effects. It would also be ideal to have large number of trials to improve on accuracy but is impractical due to the time constraint. Calculations in this study will continue within the limitations of the simulation (Rytov<0.9).

Knowing that the phase variance approaches the value that is near the theoretical approach, we can proceed to determining the autocorrelation at different levels of turbulence defined by Rytov. The auto-correlation is calculated for phase screens at the receiving end that have a phase variance near the theoretical. The ideal case would be determining an ensemble average of all the autocorrelation values within each simulation. This would lead to storing 20, 2048x2048 matrices, which is not appropriate given the length of this study.

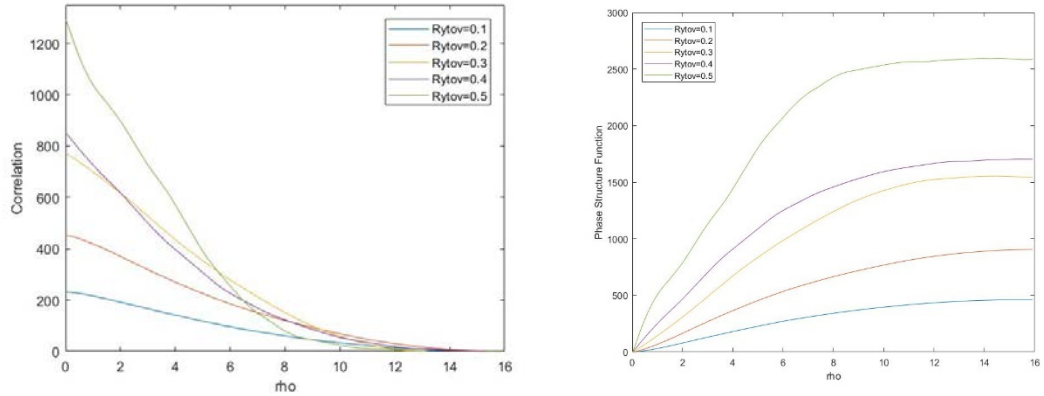

Figure 6: Phase Autocorrelation & Structure Function for varying values of Rytov

Autocorrelation values is calculated for a 2-D plane but only a vector from the center of the plane in the positive x-axis is used to plot (Fig 6.). This is done for simplicity and to compare to 1-D calculated values of the phase structure function. The slope of each autocorrelation decreases exponentially before approaching zero. The initial value for each curve is equivalent to its respective phase variance. Theoretically at lower levels of turbulence, the autocorrelation should approach zero faster than that of higher levels. This is true for autocorrelation values between the range of $0.1 \leq Rytov \leq 0.3$. The autocorrelation values decline faster than predicted for the finite grid simulations at Rytov≥0.4. On the other hand, the structure function begins increasing quadratically but begins to bend over as the spacing increases before it saturates to twice the phase variance.

To evaluate the simulated structure function, we need to calculate the phase structure function established by Tatarskii [7].

$$D_{\varphi}(\rho) = 8\pi^2 L k^2 \int_0^{\infty} \kappa \Phi_n(\kappa)\left[1 - J_o(\kappa\rho)\right] d\kappa$$

In this equation $J_o(\kappa\rho)$ is the wavenumber weighting function and the structure function can be derived for various models of the power spectrum. The structure function using the Kolmogorov model approaches an asymptotic value. Meanwhile the von Kármán saturates more rapidly and approaches the asymptotic value smoothly. We use these results to interpret the simulated data.

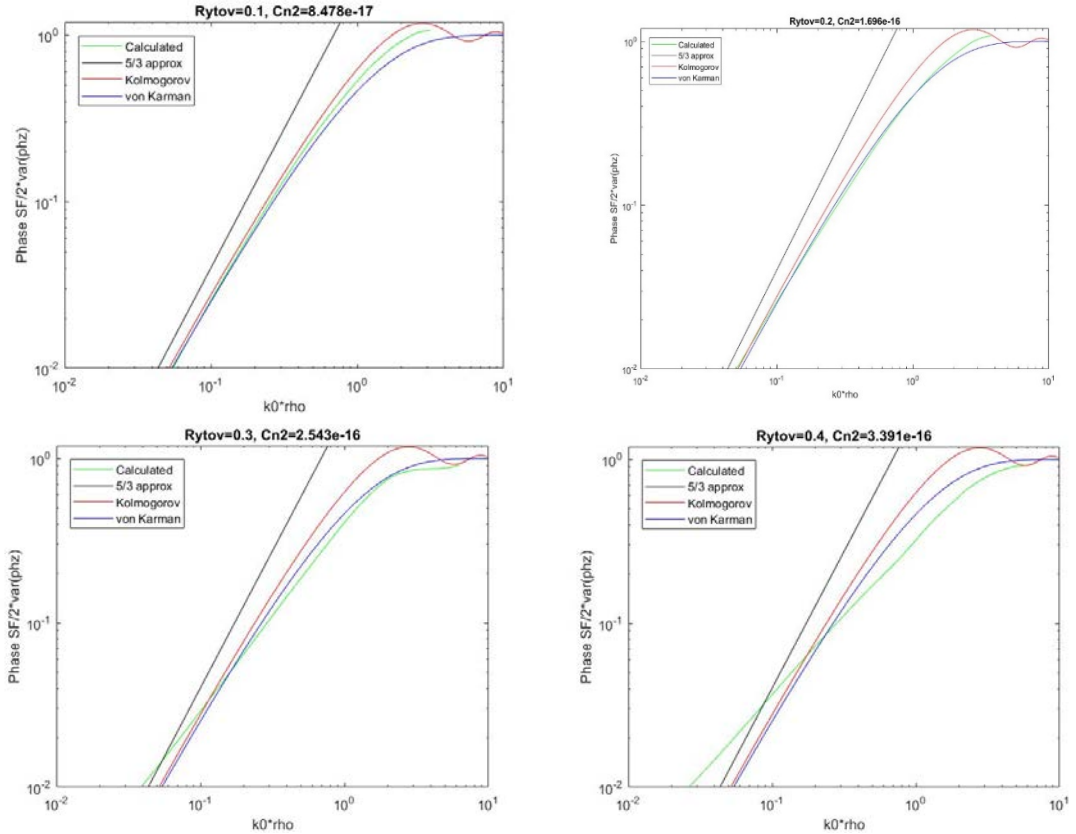

Figure 7: Phase Structure Function compared to calculated values

Progressing from phase variance to the phase structure function, limitations of using a finite spatial grid become more prominent at Rytov≥0.4. Rytov values above this range will still

saturate at the asymptotic value but does not retain the shape of the theoretical von Kármán calculation. Within the range of $0.1 \leq Rytov \leq 0.3$, the phase structure function is approximately same as the calculated theoretical values. Structure Function in Rytov values 0.1 and 0.2 range are initially like the von Kármán before overshooting the asymptotic value. The structure function at Rytov=0.3 is not as smooth as the previous two and doesn't match the von Kármán initially but remains a good approximation at $\kappa_o \rho > .1$. Currently, we can only characterize laser propagation at low turbulence. This does not mean the Kolmogorov model breaks apart at high turbulence but further investigations are needed. With High Performance Computing (HPC), we can begin simulation with a screen size large enough that will allow for deep turbulence effects for a laser propagating over a long path.

5 CONCLUSION

Unlike the variance of intensity, the phase variance does not saturate with respect to Rytov which allowed for further calculations of phase autocorrelation and structure function. We have noticed the dependence of phase trends to larger eddies in the calculation. HPC can allow us to simulate a spatial phase screen size that is significantly larger than the outer scale length so the sample frequency spacings can accurately represent phase data at high turbulence. This will allow for future investigation of characterizing deep turbulence effects through the phase variance. Further investigations using non-Kolmogorov descriptions can also help us better understand the deep turbulence effects and develop better metrics for the laser propagation.

6 ACKNOWLEDGEMENT

The study was supported by the U.S. Air Force through the 2017 Summer Faculty Fellow Program (SFFP). I would like to acknowledge the Air Force, AFRL RDSM, Maui High Performance Computing Center (MHPCC), and System Plus. I would also like to include a special thanks to our AFRL mentor Dr. V.S. Rao Gudimetla, and Clarence Brown at System Plus.

7 REFERENCES

[1] A. Kolmogorov, *In Turbulence, Classic Papers on Statistical Theory*. New York: Interscience, 1961.

[2] L. A. Chernov, *Wave propagation in a random medium. Translated from the Russian by R. A. Silverman*. New York: McGraw-Hill, 1960.

[3] V. I. Tatarskii, *The Effects of the Turbulent Atmosphere on Wave Propagation*. Springfield: National Technical Information Service U.S. Dept. of Commerce, 1971.

[4] R. L. Phillips and L. C. Andrews, "Measured statistics of laser-light scattering in atmospheric turbulence," *J. Opt. Soc. Am.*, vol. 71, no. 12, p. 1440, 1981.

[5] A. Consortini, F. Cochetti, J. H. Churnside, and R. J. Hill, "Inner-scale effect on irradiance variance measured for weak-to-strong atmospheric scintillation," *J. Opt. Soc. Am. A*, vol. 10, no. 11, p. 2354, 1993.

[6] A. Wheelon, *Electromagnetic Scintillation I. Geometrical Optics*, 1st ed. New York: Combridge University Press, 2001.

[7] G. Weiss, "Wave Propagation in a Turbulent Medium. V. I. Tatarski. Translated by R. A. Silverman. McGraw-Hill, New York, 1961. 285 pp. Illus. $9.75," *Science (80-.).*, vol. 134, no. 3475, pp. 324–325, Aug. 1961.

[8] J. W. Strohbehn, "Line-of-sight wave propagation through the turbulent atmosphere," *Proc. IEEE*, vol. 56, no. 8, pp. 1301–1318, 1968.

[9] V. Kumar, “Laser beam propagation through a long path: Developing new metrics for deep turbulence effects,” *SFFP report - DTIC*. 2016.
[10] J. D. Schmidt, *Numerical Simulation of Optical Wave Propagation with Examples in MATLAB*. 2010.
[11] D. C. Ghiglia Pritt, M.D., D. Ghiglia, and M. Pritt, *Two-Dimensional Phase Unwrapping: Theory, Algorithms and Software*. 1998.
[12] R. M. Goldstein, H. a Zebker, and C. L. Werner, “Satellite radar interferometry: Two-dimensional phase unwrapping,” *Radio Sci.*, vol. 23, no. 4, pp. 713–720, 1988.
[13] C. Smith, “GoldsteinUnwrap2D_r1.” MATLAB 7.11 (R2010b), 2010.